

## PHYSICAL PROPERTIES OF THE SKYLAB NORTH POLAR CORONAL HOLE WITH AN EXTENDED BASE AND ITS MHD SELF-CONSISTENT MODELLING

S. Bravo and G. Ocaña

Instituto de Geofísica  
Universidad Nacional Autónoma de México

1990 July 31

### RESUMEN

Con base en las observaciones del Skylab del Sol en rayos X que permitieron estimar la forma de la frontera del hoyo coronal del polo norte y en las observaciones de luz blanca que permitieron derivar un perfil de densidad para el flujo de viento solar proveniente de ese hoyo, Munro y Jackson (1977) concluyeron que se requiere una adición substancial de energía al flujo hasta al menos  $5 R_{\odot}$ . En este trabajo, recalculamos los perfiles de velocidad y de temperatura para el mismo hoyo pero considerando una frontera diferente que es más ancha en la base, de acuerdo con las observaciones del coronómetro-K del HAO, los espectroheliogramas en EUV del OSO-7 y las fotografías de la corona solar cerca de los 4500 Å. Se tomaron también las incertidumbres en el perfil de densidad electrónica inherentes a las observaciones de luz blanca y se consideraron diversos valores posibles del flujo de masa 1 UA. Encontramos que las diferencias introducidas no son suficientes para descartar la necesidad de una energización extensa del viento solar, pero una de las soluciones posibles muestra una concordancia muy buena con el modelado MHD autoconsistente del flujo con el único término adicional de la fuerza de Lorentz en la ecuación de momento.

### ABSTRACT

Based on the near to the Sun boundary of the Skylab north polar coronal hole estimated from the AS & E X-ray photographs and on the density profile deduced from white light data, Munro and Jackson (1977) concluded that substantial energy addition to the solar wind flux is required up to at least  $5 R_{\odot}$ . In this paper we recalculate the velocity and temperature profiles for the same hole but considering a different boundary for the flux tube which is larger at its base, according to the HAO K-coronameter observations, the OSO-7 EUV spectroheliograms and pictures of the solar corona near 4500 Å. We also take into account the uncertainties inherent in the white light observations leading to the electron density profile and consider different possible values of the solar wind mass flux at 1 AU. We find that the differences introduced are not sufficient to discard the necessity of an extended energization of the wind, but one of the possibilities allowed for the flux within the observational uncertainties shows a very good agreement with an MHD self-consistent modelling with the only additional term of the Lorentz force in the momentum equation.

*Key words:* SUN-CORONA

### 1. INTRODUCTION

Although the physics of the solar wind is well understood in general terms since the early work of Parker (1958, 1963, 1964a,b, 1965), some problems still remain unsolved. One of them concerns the acceleration of the wind, specially in the high speed streams emanating from large coronal holes which seem not to be accounted for by a simple thermal conductive expansion. Munro and Jackson (1977) made an extensive study of the physical properties

of the Skylab north polar coronal hole by using the observations of the electronic density profile at the corona and of the shape of the coronal hole flux tube to calculate the velocity and temperature profiles from 2 to  $5 R_{\odot}$ . They used the observations of the High Altitude Observatory's white light coronagraph on Skylab to determine the density structure within the hole and the AS & E X-ray photographs of the corona to estimate the shape of the boundary of the hole near the solar surface.

They also considered the mass flux of the solar wind at 1 AU to be  $3 \times 10^8 \text{ cm}^{-2} \text{ s}^{-1}$  as measured on the ecliptic near the Earth. By using all this information they were able to determine the actual velocity profile along a flux line in the coronal hole for a stationary situation and used it to obtain temperature profiles. From their analysis they conclude that energy—as thermal energy and/or momentum addition—must be deposited in the solar wind at least from 2 to beyond  $5 R_s$ .

However, a latitudinal variation of the interplanetary Lyman  $\alpha$  distribution has been observed and it has been interpreted as implying a 30-50% decrease in the solar wind mass flux from solar equator to pole during much of the period between 1973 and 1977, when large polar coronal holes dominated the large-scale solar coronal structure (Kumar and Broadfoot 1979; Lallement *et al.* 1985). That means that the mass flux of the high-latitude solar wind associated with large polar coronal holes is considerably less than that of the solar wind in the ecliptic plane.

Lallement *et al.* (1986) re-examined the analysis of Munro and Jackson (1977) of the Skylab north polar coronal hole taking into account such variation in the mass flux value and giving attention also to the uncertainties inherent in the estimation of the electron density radial profile inferred from coronal white light observations which increase with distance and at  $5 R_s$  can be as large as about one order of magnitude. From their recalculations of the velocity and temperature profiles in a parametric study within the allowed ranges for the solar wind mass flux at 1 AU and the coronal electron density profile, Lallement *et al.* (1986) conclude that it is not definite that a considerable amount of energy must be deposited in the lower corona as the profiles obtained are consistent with both the necessity of a substantial energy addition and to the absence of any significant addition of energy in the region observed.

In a recent paper, Bravo and Mendoza (1989) have shown that a better estimation of the Skylab north polar coronal hole boundary is obtained when considering the corresponding HAO ground-based K-coronameter data which agree with the border estimated by Koutchmy (1977) using the pictures of the solar corona obtained near 4500 Å during the 30 June, 1973 solar total eclipse. This border shows a wider extension near the solar surface than the one estimated by Munro and Jackson and so leads to different velocity and temperature profiles for the solar wind near the Sun. It is the purpose of this paper to recalculate such profiles, within the frame of the considerations made by Lallement *et al.* (1986), but in terms of the wider boundary of the Skylab north polar coronal

hole and to compare the results with those obtained from an MHD self-consistent model worked out by Robertson (1983) for the Skylab hole.

## II. THE GEOMETRY OF THE SKYLAB NORTH POLAR CORONAL HOLE

In their study of the Skylab north polar coronal hole, Munro and Jackson (1977) used the Kopp and Holzer (1976) expression for the cross sectional area of the flux tube of a coronal hole

$$A(r) = (A_0/r_0^2) r^2 f(r), \quad (1)$$

where  $A_0$  is the cross sectional area of the flux tube at  $r_0$  (namely the base of the corona),  $r$  is the distance to the centre of the Sun, and  $f(r)$  is a function which accounts for the more than radial expansion. This function is given by

$$f(r) = (f_{max} E + f_1)/(E + 1); \quad (2)$$

where

$$E = \exp [(r - r_1)/\sigma],$$

$$f_1 = 1 - (f_{max} - 1) \exp[(r_0 - r_1)/\sigma],$$

and the values of  $f_{max}$ ,  $\sigma$ , and  $r_1$  adjust to the specific geometry.

As seen from these expressions,  $f(r)$  attains the maximum value  $f_{max}$  at a certain distance from the Sun, where the flux from the hole becomes radial, and remains practically constant farther out. In the Munro and Jackson model  $f_{max}$  has a value of 7.26 and it is almost achieved at a distance of 3-4  $R_s$ . This means that when the radial expansion begins the cross sectional area of the flux tube is 7.26 times greater than that obtained for the case of a radial expansion all the way from the base of the corona.

In the analysis of Bravo and Mendoza (1989), the area of the Skylab north polar coronal hole turns out to be much wider near the solar surface than that estimated by Munro and Jackson and so the cross sectional area of the hole at 3  $R_s$  is only about 2.9 times greater than that obtained from a purely radial expansion. This wider border can also be represented by the Kopp and Holzer expression mentioned above when using the following values for the specific parameters:

$$f_{max} = 4.5; r_1 = 0.8 R_s; \sigma = 0.7 R_s; A_0 = 1.02 R_s^2.$$

The good fit of this expression to the actual border of the hole as observed with the HAO ground-based K-coronameter and from the OSO-7 EUV spectroheliograms is shown in Figure 1. For the analytical adjustment, the left side border of the observed hole was considered to represent an axially symmetric hole; this border is nowhere

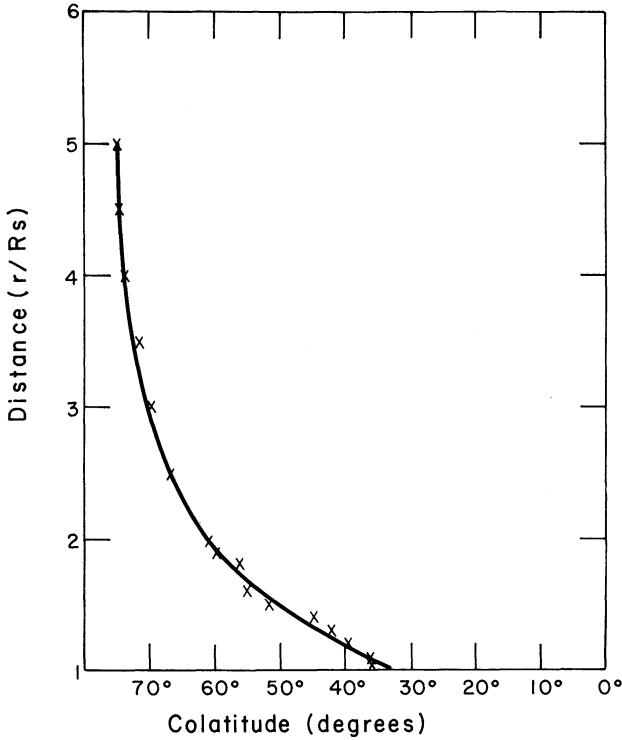


Fig. 1. Comparison of the boundary of the Skylab north-polar coronal hole as derived from coronagraph and-HAO ground-based K-coronameter data (crosses) and the border fitted with the analytical expression in this paper (solid line).

the same as that obtained from the expression of Munro and Jackson which runs all the way inside the observational border used here.

### III. VELOCITY AND TEMPERATURE PROFILES WITH THE EXTENDED BASE

We can now use the corrected geometry of the Skylab north polar coronal hole flux tube described above to compute the actual velocity profile at the centre of the hole by means of the continuity equation for a stationary situation

$$N(r) v(r) A(r) = \text{const.} \quad (3)$$

by assuming that an infinitesimal flux tube at the pole has the same geometry of expansion as the whole flux tube from the polar hole. Here,  $N(r)$  represents the electron density and  $v(r)$  the velocity of the expansion.

Such a computation requires also the knowledge of the coronal radial electron density profile at the Sun's pole and of the mass flux at some place within the flux tube, namely at 1 AU. For the latter we shall consider here both the value used by Munro and Jackson of  $3 \times 10^8 \text{ cm}^{-2} \text{ s}^{-1}$  as well as the smaller value, more appropriate to polar regions,

of  $1 \times 10^8 \text{ cm}^{-2} \text{ s}^{-1}$  obtained from Lyman  $\alpha$  observations. With respect to the electron density profile we shall take the medium and flattest profiles from Lallement *et al.* (1986) (profiles A and C in their paper) as they explicitly discard the steepest one for leading to unrealistically high velocities of the solar wind near the Sun. Each density profile is represented analytically by a polynomial fit of the form

$$N(r) = \sum_i (a_i r^{-b_i}).$$

The specific values of the coefficients  $a_i$  and  $b_i$  for both profiles can be found in their paper.

In Figures 2a and 2b we have drawn the velocity profiles obtained from the above considerations. The velocity profiles derived by Lallement *et al.* (1986) using the Munro and Jackson (1977) geometry are also drawn for comparison. As expected, the velocity profiles for the extended hole are lower.

In order to analyze the energy requirements of such expansion we calculated also the temperature profiles corresponding to each one of the velocity profiles assuming that the only driving force is the one due to the thermal pressure gradient. In this case the momentum equation is

$$v dv/dr = -1/\rho dP/dr - GM_s/r^2 \quad (4)$$

where  $\rho$  is the mass density of the solar wind plasma,  $P$  is the pressure taken as  $P = 2NkT$ ,  $G$  the universal gravitation constant, and  $M_s$  the Sun's mass. We have considered a purely hydrogen plasma and do not assume any addition of momentum by hydromagnetic waves or any other source. Although the magnetic force is not considered in the momentum equation, the effect of the magnetic field is somehow included in the velocity profiles which are determined by the observed characteristics of the flux tube of the hole which in turn are modulated by the presence of the field.

From equation (4) we have the following equation for the temperature:

$$d(\rho T)/dr = (-\rho m_H/2k) (v dv/dr + GM_s/r^2) \quad (5)$$

where  $m_H$  is the proton mass,  $k$  is the Boltzmann constant, and  $\rho(r)$ ,  $v(r)$ , and  $dv(r)/dr$  are now known functions. By taking the integral of this equation from a certain point  $r$  near the Sun to  $r = 5 R_s$  we obtain

$$T(r)\rho(r) = (T\rho)_{5R_s} + (m_H)/(2k) \times \int_r^{5R_s} \rho(v dv/dr + GM_s/r^2) dr \quad (6)$$

The integration of equation (6) was performed numerically for different values of  $T_{5R_s}$  and the temperature profiles obtained with the values of

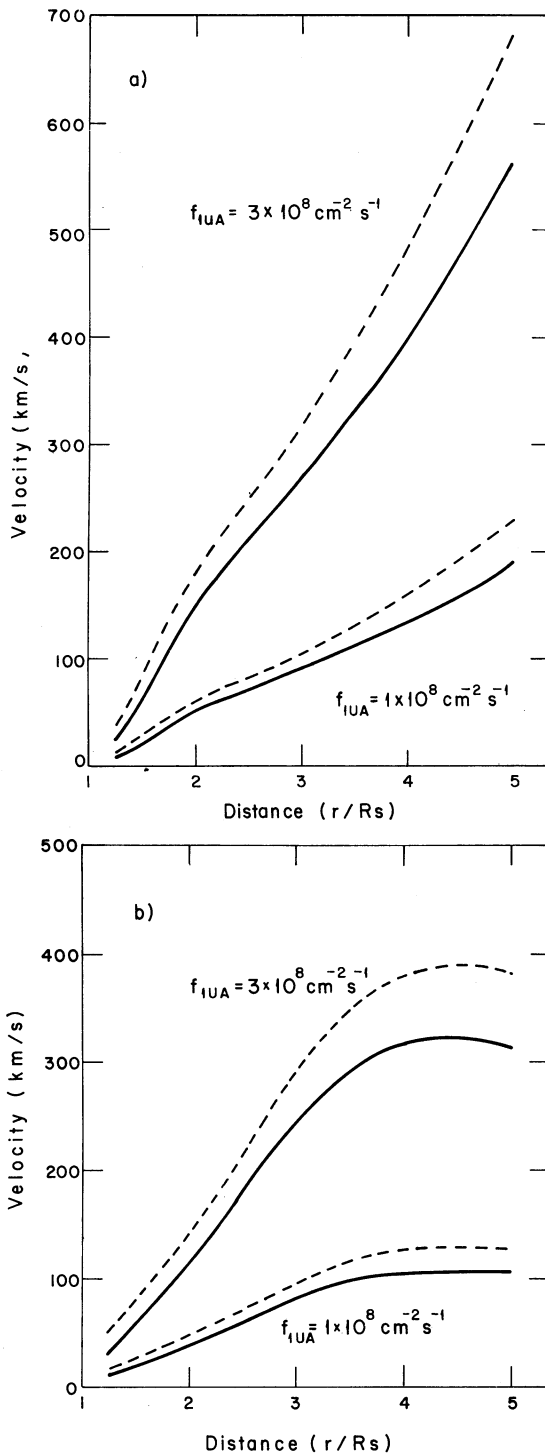


Fig. 2. Flow speed,  $v$ , versus heliocentric radial distance,  $r$ , for two values of the mass flux density at 1 AU, namely  $10^8$  and  $3 \times 10^8 \text{ cm}^{-2} \text{ s}^{-1}$ . The solid lines represent the profiles calculated with our broader geometry and the dashed lines those obtained by Lallement *et al.* (1986) using Munro and Jackson's geometry. Figures (a) correspond to their density profile A, and figures (b) to their density profile C.

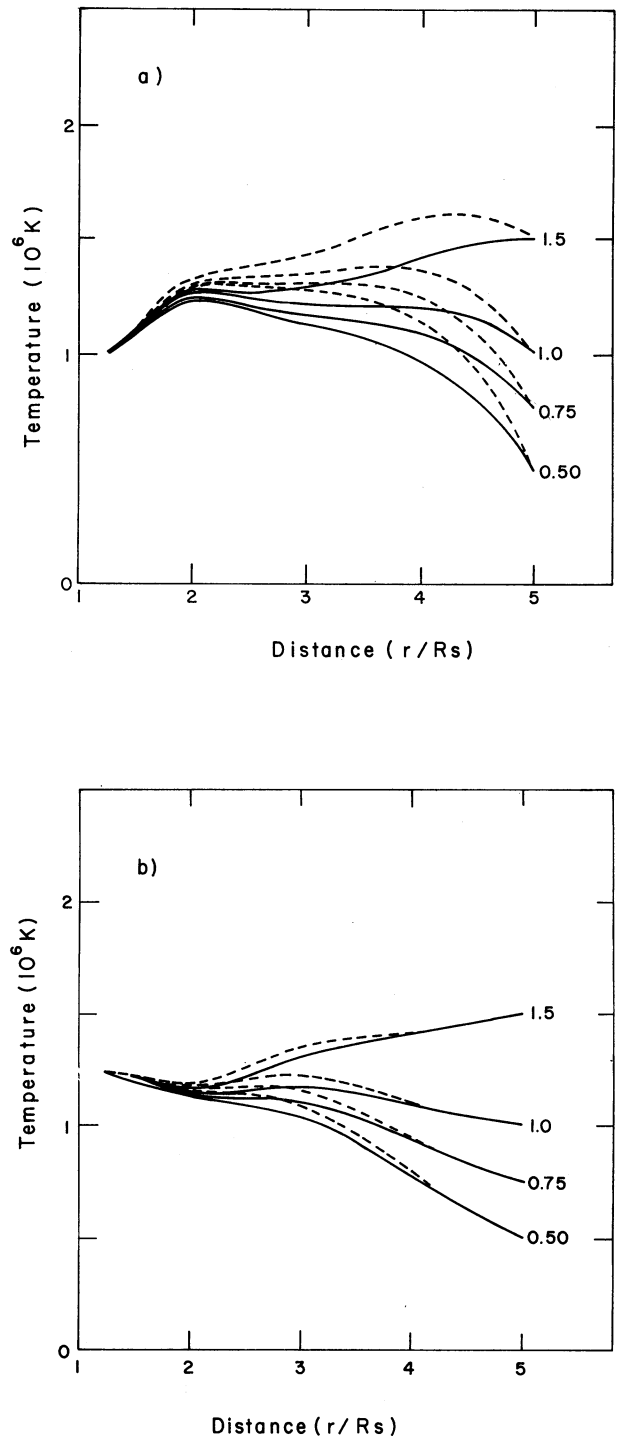


Fig. 3. Radial temperature profiles corresponding to different boundary values of  $T$  at  $5 R_s$  for density profiles A (Figure 3a) and C (Figure 3b), and for a proton flux density of  $10^8 \text{ cm}^{-2} \text{ s}^{-1}$  at 1 AU. Solid curves represent the profiles derived from our corrected geometry and dashed curves those obtained by Lallement *et al.* (1986).

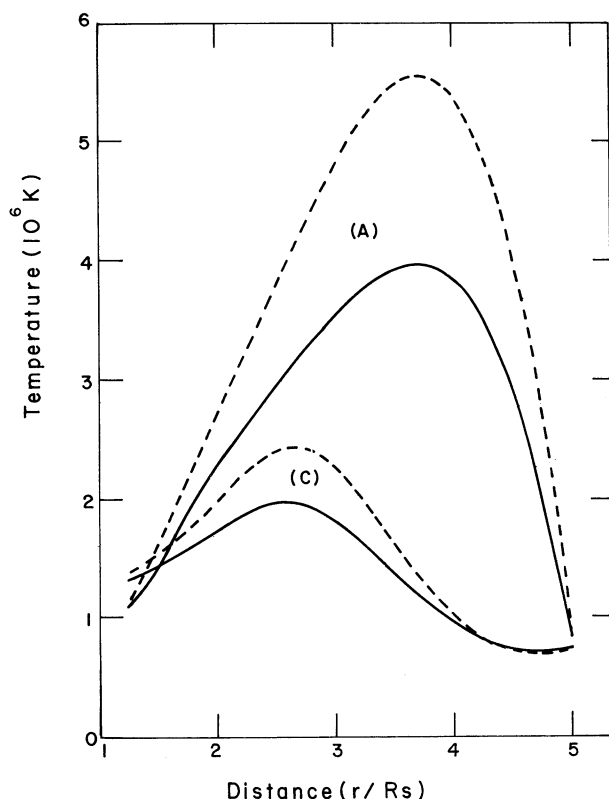


Fig. 4. The same temperature profiles as in Figure 3 but for a proton flux density at 1 AU of  $3 \times 10^8 \text{ cm}^{-2} \text{ s}^{-1}$  and for  $T(5 R_s) = 0.75 \times 10^6 \text{ K}$ .

$1 \times 10^8$  and  $3 \times 10^8 \text{ cm}^{-2} \text{ s}^{-1}$  for the mass flux of the solar wind at 1 AU are drawn in Figures 3a and 3b and in Figure 4, respectively. In Figures 3a and 3b, two families of curves are shown, one corresponding to the Munro and Jackson geometry and the other to the geometry described here; Figure 3a corresponds to the density profile A in Lallement *et al.* (1986) and Figure 3b to their profile C. In Figure 4 the temperature profiles obtained for the condition  $T = 0.75 \times 10^6 \text{ K}$  at  $r = 5 R_s$  are shown for both density profiles (A and C). The profiles corresponding to other temperatures at  $5 R_s$  were omitted because they are almost identical to the one shown with exception of the very end of the line where each one meets its corresponding boundary condition.

As can be seen from the figures, although the curves with the broader border are always lower, the difference is not sufficient to remove the ambiguity pointed out by Lallement *et al.* (1986) with respect to the necessity of additional energization of the flux at large distances from the Sun. When using the larger value within the observational uncertainties of the proton flux density at 1 AU, the

new temperature profiles also show an increase at very high temperatures which requires either an additional energy supply extended to large distances to account for such increase or the inclusion in the momentum equation of an additional term (for example, an Alfvén wave pressure gradient) whose effect would be the reduction of the magnitude of the thermal pressure gradient force required to drive the observationally inferred flow and thus reduce the inferred coronal temperature. In contrast, density profile C with a proton flux density at 1 AU of  $1 \times 10^8 \text{ cm}^{-2} \text{ s}^{-1}$  leads to a temperature that decreases nearly monotonically with increasing radius and thus does not require any significant energy addition in the observed region.

#### IV. COMPARISON OF THE NEW PROFILES WITH THE RESULTS OF AN MHD SELF-CONSISTENT MODELLING

As pointed out earlier by Bravo and Mendoza (1989), the border of the Skylab north polar coronal hole obtained from coronagraph and EUV observations worked out in this paper coincides very well with the border obtained from the MHD self-consistent simulation of the flux in this hole carried out by Robertson (1983) and corresponds very closely to a dipole field-like expansion. Robertson employed the numerical iterative technique developed by Pneuman and Kopp (1971) to integrate the highly non-linear system of differential equations which describe the plasma-magnetic field coupling governing the flux. He modified and extended the method of solution to describe a thermally conductive plasma and used the classical expression for the thermal conductivity in a collision-dominated plasma given by Spitzer (1962). He assumed a value of  $2.25 \times 10^8 \text{ cm}^{-2} \text{ s}^{-1}$  for the mass flux of the solar wind at 1 AU on the polar axis.

In his work, Robertson was able to calculate the overall magnetic field configuration in the hole as well as the density, velocity, and temperature radial profiles for different latitudes from the centre to the border of the hole. In Figure 5 we have drawn his density profile corresponding to the polar axis along with the C profile from Lallement *et al.* (1986); as can be seen, a good agreement is obtained except in the region nearest to the Sun. As the density profile and the geometry of the flux tube look very similar to the ones used in this paper, a satisfactory agreement can be expected in the velocity profiles. In Figure 6, Robertson's velocity profile for the pole and the one obtained in this paper for profile C and a flux mass at 1 AU of  $1 \times 10^8 \text{ cm}^{-2} \text{ s}^{-1}$  are shown; the resemblance of the profiles is quite good except for the fact that Robertson's velocities are higher. This is a consequence of the choice he made for the mass flux



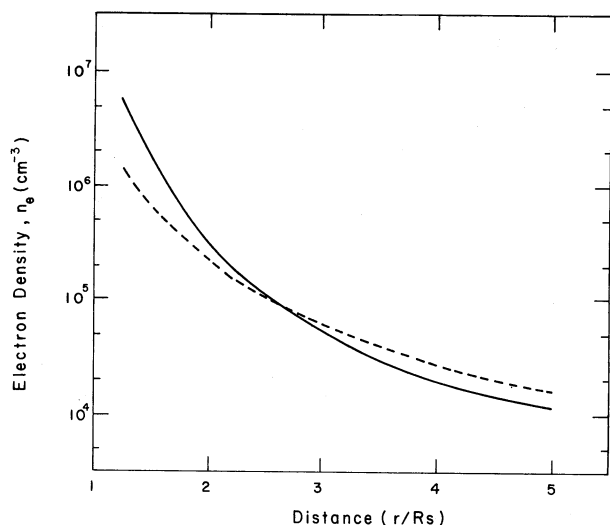


Fig. 5. Density profile C from Lallement *et al.* (1986) (solid line) compared with that obtained from the Robertson's (1983) self-consistent MHD model of the Skylab north polar coronal hole at the pole (dashed line).

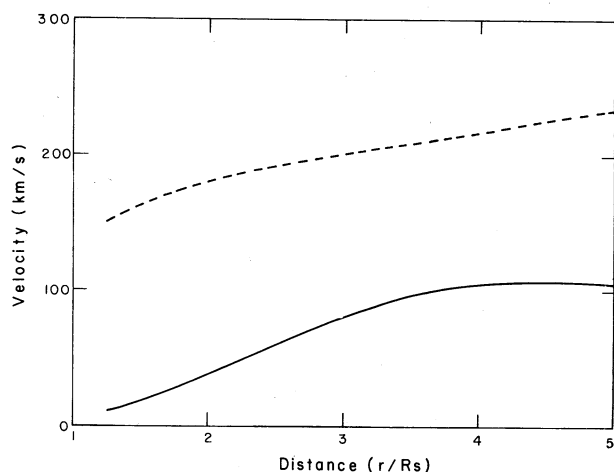


Fig. 6. Our flow speed profile corresponding to density profile C and to a proton flux density at 1 AU of  $10^8 \text{ cm}^{-2} \text{ s}^{-1}$  compared with that obtained in Robertson's (1983) model for the pole.

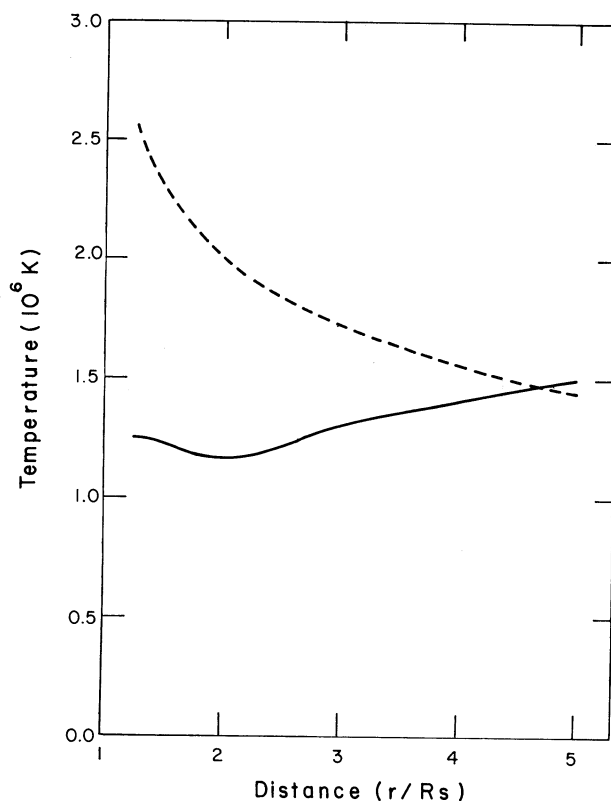


Fig. 7. Robertson's radial temperature profile at the pole (dashed line) compared with ours for the density profile C and with a proton flux density of  $10^8 \text{ cm}^{-2} \text{ s}^{-1}$  at 1 AU (solid line).

only consider pressure gradient and gravitational forces, Robertson includes also the magnetic force.

## V. DISCUSSION AND CONCLUSIONS

The main conclusion of this study is that the actual characteristics of the Skylab north polar coronal hole, mainly its overall geometry and its plasma and magnetic field flux, can be satisfactorily reproduced by an MHD self-consistent model when considering the border with the extended base. Even when the density and velocity profiles obtained by Robertson do not correspond precisely to those observationally derived, it seems possible to adjust them by simply considering equal boundary values. Although in the case of the temperature profiles the situation is not clear, the main difference may arrive from the introduction of the magnetic field in Robertson's modelling and not considered in this paper. However, the heat conduction expression used by Robertson could also be a source of discrepancy as he took Spitzer's expression for collision-dominated plasmas all the way to the Earth while the solar wind becomes a collisionless plasma not too far from the

of the solar wind at 1 AU which was  $2.25 \times 10^8 \text{ cm}^{-2} \text{ s}^{-1}$ . It might be expected that when using in his model a lower value, such as that of Lallement *et al.* a better fit could be obtained.

With respect to the temperatures, Robertson's profile is quite different from the corresponding one in this paper (see Figure 7). This is not surprising because the assumptions made in the momentum equation are quite different: while we

Sun. In any case it is clear that this kind of modeling is very promising and that further work on it is worthwhile.

#### REFERENCES

- Bravo, S. and Mendoza, B. 1989, *Ap. J.*, **338**, 1171.  
 Kopp, R.A. and Holzer, T.E. 1976, *Solar Phys.*, **49**, 43.  
 Koutchmy, S. 1977, *Solar Phys.*, **51**, 399.  
 Kumar, S. and Broadfoot, A.L. 1979, *Ap. J.*, **228**, 302.  
 Lallement, R., Bertaux, J.L., and Kurt, V.G. 1985, *J. Geophys. Res.*, **90**, 1413.  
 Lallement, R., Holzer, T.E., and Munro, R.H. 1986, *J. Geophys. Res.*, **91**, 6751.  
 Munro, R.H. and Jackson, B.V. 1977, *Ap. J.*, **213**, 874.  
 Parker, E.N. 1958, *Ap. J.*, **128**, 664.  
 Parker, E.N. 1963, *Interplanetary Dynamical Processes*, (New York: Interscience Publ.).  
 Parker, E.N. 1964a, *Ap. J.*, **139**, 72.  
 Parker, E.N. 1964b, *Ap. J.*, **139**, 93.  
 Parker, E.N. 1965, *Space Sci. Rev.*, **4**, 666.  
 Pneuman, G.W. and Kopp, R.A. 1971, *Solar Phys.*, **18**, 258.  
 Robertson, B.J. 1983, *Solar Phys.*, **83**, 63.  
 Spitzer, L. 1962, *Physics of Fully Ionized Gases*, (New York: Interscience Publ.)

Silvia Bravo and Gerardo Ocaña: Instituto de Geofísica, Depto. de Física Espacial, UNAM, Coyoacán 04510, D.F., México.